Nacelle Integration Study on a Mach-2.2 Supersonic Cruise Aircraft

H.R. Welge,* R.L. Radkey,† and P.A. Henne‡
McDonnell Douglas Corporation, Long Beach, Calif.

Results of a propulsion system integration study performed on a Mach-2.2 advanced supersonic cruise aircraft are discussed. A study configuration developed in a joint NASA-Douglas supersonic technology program was used as the baseline airframe to study the detailed problems of inlet-nacelle-airframe integration at Mach 2.2. Numerous inlet-nacelle combinations were examined in a preliminary screening study. Promising configurations were evaluated in a nacelle installation study in which structural weight and installed wave drag were traded leading to the selection of an axisymmetric single-engine pod installation as the most promising configuration. A detailed nacelle shape study was conducted, and a wing reflex was designed. A cooperative NASA-Douglas wind-tunnel test of the refined nacelle with both mixed and external compression inlets was conducted with the nacelles installed on both a refined baseline wing and a reflexed wing. An installation drag penalty equal to 4.3% of the baseline wing-body drag was observed for the external compression inlet over the mixed compression inlet. Wing reflexing improved the trimmed wing-body-nacelle drag by 3.0% of the wing-body drag. Good agreement was observed between calculated and experimental increments in induced drag due to nacelle installation.

Introduction

INTEREST has been renewed both at NASA and in industry in conducting technology-assessment studies on supersonic cruise aircraft. One of the basic tasks has been to identify, through aircraft design studies, the key technologies that must be pursued to reduce operating costs, meet environmental constraints, and improve efficiency for second-generation supersonic cruise configurations. The Douglas Aircraft Company began these studies by reassessing the selection of cruise Mach number. It was found that Mach 2.2 provided the best mix of low operating costs, high revenue productivity, near-term technology materials, and low program risks for typical four-engine transport configurations.[1]

The development of a technology-assessment baseline wing-body configuration, shown in Fig. 1, required detailed support from many technical disciplines. As discussed in recently completed NASA Systems Studies,[2,3] the baseline configuration was derived through extensive study and features an arrow wing with an optimized wing area integrated with a fuselage optimized for minimum wave drag. The sum of the wing structural weight and drag equivalent weight was minimized by tailoring the wing-thickness distribution and by optimizing the structural arrangement with attention to strength, fail-safe, aeroelastic, and flutter criteria and by using advanced structural concepts. All significant subsystems were examined in detail, and an advanced supersonic technology engine with exhaust noise suppression and acoustic treatment was identified for use as a baseline study engine. The selection of the baseline configuration raised many questions concerning proper inlet-nacelle-airframe integration for such a design.

The nacelle design selected for the Mach-2.7 U.S. SST program (1971) featured axisymmetric mixed compression inlets installed on single-engine axisymmetric nacelles. The demand for maximum aerodynamic efficiency at the higher Mach number of 2.7 dictated mixed compression inlets. The lower cruise Mach number of the Douglas studies required the reexamination of the performance potential of numerous aerodynamic design alternatives. The results of the inlet-nacelle-airframe design and integration studies are presented in this paper.

Four studies were conducted. The first was a screening study of numerous inlet-nacelle combinations. This study identified three alternatives having significant performance advantages. These arrangements were further evaluated in the second study, a nacelle installation study. This study resulted in the selection of an axisymmetric single-engine nacelle for the third study, a detailed design and integration study including the design of a reflexed wing. Because no clear analytic preference could be shown for either a mixed or external compression inlet on the axisymmetric nacelle and because it was considered important to evaluate the analyses and conclusions of these studies, a fourth study, a wind-tunnel test of the two inlet-nacelle arrangements including the effects of wing reflexing, was conducted.

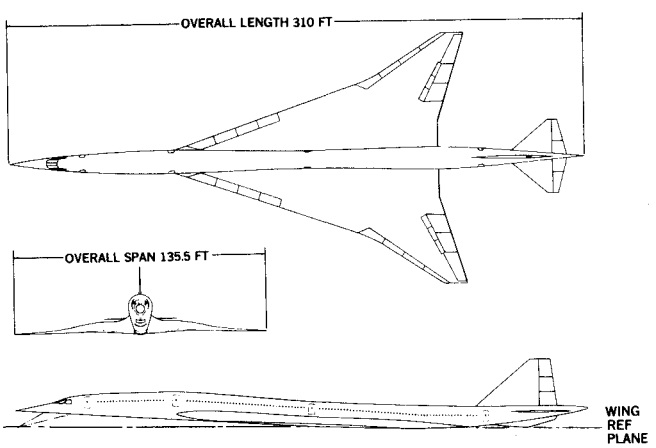

Fig. 1 AST baseline configuration—1973.

Presented as Paper 76-757 at the AIAA/SAE 12th Propulsion Conference, Palo Alto, Calif., July 26-29, 1976; submitted Oct. 4, 1976; revision received July 18, 1977.

Index categories: Power Plant Design; Configuration Design; Aerodynamics.

*Unit Chief, Aerodynamics Subdivison, Douglas Aircraft Company. Associate Fellow AIAA.

†Engineer/Scientist Specialist, Aerodynamics Subdivision, Douglas Aircraft Company.

‡Engineer/Scientist Specialist, Aerodynamics Subdivision, Douglas Aircraft Company. Member AIAA.

It is important to note that for a detailed study such as this, the analysis must be tied to a specific configuration in order to achieve meaningful, realistic answers to the problems of wing-nacelle integration. The detailed designs resulting from this or any similar study are, however, transitory in nature as configuration refinements can be made ad infinitum. Consequently, this paper focuses on the generally applicable methods of analysis, techniques of design, and technical conclusions resulting from this program.

Inlet-Nacelle Screening Study

The purpose of the inlet-nacelle screening study was to make a first-order comparison of a variety of different configurations prior to detailed integration with the airframe. This comparison served to identify those configurations having higher performance potential and deserving more detailed analysis. Ten inlet configurations, including axisymmetric and two-dimensional designs with both external compression and mixed compression, were considered. Engine installations included single-engine, dual-engine, and quadruple-engine nacelles. Twenty-two inlet-nacelle configurations were compared. Unreasonable configurations such as a quadruple-engine nacelle with axisymmetric inlets were eliminated.

Analysis was performed assuming Mach 2.2 at the inlet face. Inlet total pressure recovery, nacelle external skin friction drag, inlet boundary-layer bleed drag, subcritical spillage drag, and inlet weight were estimated for each configuration. These estimates were made using a combination of theoretical analyses and empirical correlations with test data.

The inlet matrix is shown in Fig. 2. Inlets 1-4 are two-dimensional. Inlets 5-9 are axisymmetric. Inlet 10 is a symmetric or bifurcated two-dimensional inlet. All geometries are shown for the same engine compressor face diameter. The substantial length reduction of the axisymmetric inlets is obtained in the subsonic diffuser portion of the inlet. Correlations of test data[4] for annular diffusers compared to two-dimensional and conical diffusers indicate that less diffuser length is required for a given throat-to-compressor face area ratio to achieve the same compressor face Mach number and pressure recovery.

CONFIGURATION MATRIX	NUMBER EXTERNAL COMP SURFACES	PERCENT INTERNAL COMP	ESTIMATED RECOVERY AT 2.2M
1	2	0	0.899
2	3	0	0.925
3	2	30	0.920
4	1	60	0.917
5	2	0	0.917
6	1	30	0.917
7	1	60	0.941
8	3	0	0.945
9	2	30	0.942
10	3	0	0.925

Fig. 2 Summary of inlet matrix characteristics.

A comparison of the recoveries of inlets 2, 3, and 4 with those of inlets 7, 8, and 9 suggests that, to the accuracy of these estimates, the percentage of internal compression does not have a large effect on total pressure recovery. This is true because, as the amount of internal compression is increased, the better recovery due to reduced shock losses is offset by the poorer recovery due to increased internal wetted area. The amount of internal compression does, however, have a significant effect on the external cowl geometry as will be discussed later.

The inlet-nacelle drags, weights, and pressure recoveries were combined in a Direct Operating Cost (DOC) equation and relative DOC's were calculated for each of the 22 inlet-nacelle combinations. DOC's were calculated using the trade factors and cost estimates developed in concurrent joint Douglas-NASA studies.[1-3] Results are shown in Fig. 3. Although absolute levels of DOC are not very meaningful for these preliminary studies, the comparison of relative levels does provide some measure of the overall system performance. The single-pod, axisymmetric inlet configurations show the best performance potential. Approximately half the margin between the axisymmetric inlet configurations and the best two-dimensional inlet configurations is due to total pressure recovery and half is due to inlet weight advantages. The estimated bleed drag and subcritical spillage drag have little effect on the comparisons between configurations.

It must be noted that the results of Fig. 3 do not identify a distinct advantage for either mixed compression or external compression inlets. The external compression inlets are less complex than the mixed compression inlets but have large external cowl lip angles that can result in excessive nacelle wave drag. The mixed compression inlets have smaller cowl-lip angles and avoid excessive nacelle wave drag. This difference is examined in more detail in later studies.

Of the 22 inlet-nacelle configurations, three were selected for more detailed analysis. The single-engine axisymmetric nacelles with mixed compression inlet 7 (see Fig. 2) and external compression inlet 8 were selected for their superior performance and low relative DOC's. The reference configuration dual-engine nacelle with two-dimensional external compression inlet 2 was also selected because of its wide industry acceptance and similarity to installations on the Concorde, Tu-144, and B-1.

Nacelle Installation Study

Following the inlet-nacelle screening study, a nacelle installation study was conducted. Of the three most promising

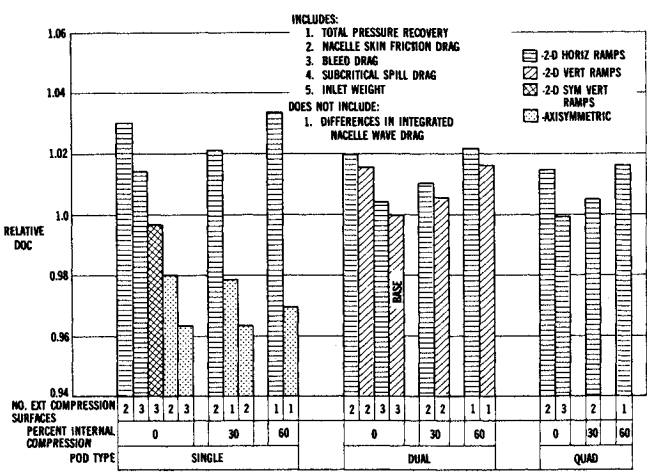

Fig. 3 Relative DOC comparison for 2.2*M* design inlet—pod study matrix.

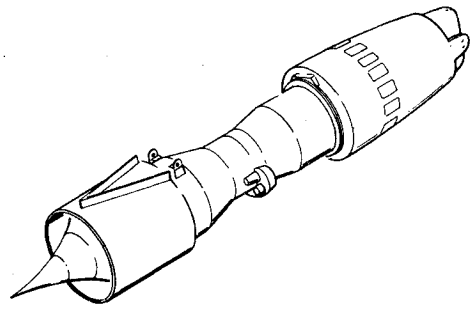

Fig. 4 Axisymmetric single-engine nacelle with external compression inlet.

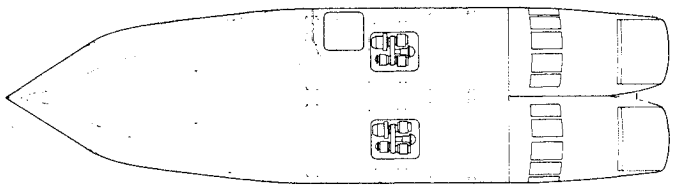

Fig. 5 Dual-engine nacelle with two-dimensional external compression inlets.

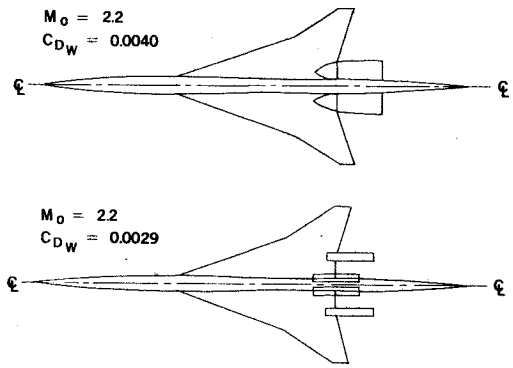

Fig. 6 Initial installation of dual-engine nacelles and single-engine axisymmetric nacelles.

inlet-nacelle combinations, two, the axisymmetric single-engine nacelle with an external compression inlet shown in Fig. 4 and the two-dimensional dual-engine nacelle with an external compression inlet shown in Fig. 5, were selected for study. It was felt that the axisymmetric nacelles with mixed compression and external compression inlets were sufficiently similar that only one need be examined. Only the installed wave drags of the various nacelle arrangements were calculated, as changes in drag due to lift were considered to be small. Configuration wave drag and structural weight were used to establish the best combination of nacelle location and wing-thickness distribution. Installed wave drag was calculated using a McDonnell Douglas developed computer program,[5] which calculates the wave drag of completely arbitrary configurations based on the area rule theory.[6,7]

Initial locations determined strictly by the lowest aerodynamic drag that could be obtained for the dual-engine two-dimensional and single-engine axisymmetric nacelles on a preliminary version of the baseline configuration wing are shown in Fig. 6. The dual-engine nacelles were installed for 11 counts more wave drag than the single-engine nacelles. This level of wave drag is an increase of 38% over that of the single-engine installation and 48% over that of the wing-body. The area rule theory $2.2M$ projected cross-sectional area distributions indicate that the nacelle area is better distributed with lower maximum wing-body-nacelle area peaks and smoother distributions for the axisymmetric single-engine nacelles than for the dual-engine nacelles. There are

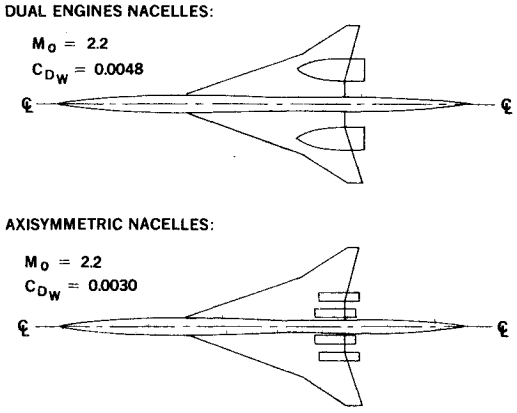

Fig. 7 Final nacelle installation following aerostructural trade study.

two primary attributes of the four-nacelle installation that make this possible. First, the nacelle area can be better distributed axially in the area rule roll angles by locating the outboard nacelles aft of the inboard nacelles and by locating the nacelles with good spanwise separation between the inboard and outboard nacelles. Second, the maximum area of two single-engine nacelles is less than the maximum area of one dual-engine nacelle.

The consideration of structural and practical constraints on the installations led to a repositioning of both the axisymmetric and the two-dimensional nacelles. The structural weight penalties associated with the far aft initial nacelle locations shown in Fig. 6 were large, and these arrangements were not compatible with landing-gear placement and ground-clearance constraints. The nacelles were relocated in a coordinated aerodynamic-structural trade study in which trades between wave drag and structural weight led to the placement of the nacelles as shown in Fig. 7.

The wave drag of each of these configurations was greater than the wave drag of the corresponding initial configurations. The new nacelle locations penalized the dual-engine nacelles more than the single-engine nacelles as the area of the dual nacelles was forced to start well ahead of the wing-body maximum area. A summary of the results of this nacelle relocation is presented in Table 1. It can be seen that the axisymmetric nacelles, as finally located, are better than the dual-engine two-dimensional nacelles in all respects except for a small increase in wetted area.

Because of the high wave drag, the dual-engine nacelle was dropped from further consideration and the nacelle integration study continued by changing the wing thickness and the wing-thickness distribution in a search for the best combination of low weight and low wave drag with the nacelles installed. Additional weight/drag trade studies were used to select new wing thickness variations, and the iterations were continued until a satisfactory combination was found. The resulting configuration had the same nacelle arrangement shown in the lower half of Fig. 7, but with a different wing thickness distribution. This new baseline configuration was used for further detailed installation studies concerned with the nacelle shape and wing-nacelle interference.

Table 1 Nacelle performance summary external compression inlet, $M_0 = 2.2$

	Single-engine axisymmetric nacelles	Dual-engine two-dimensional nacelles
ΔC_D wave due to installation	0.0003	0.0021
Increase over wing-body drag	11%	78%
Relative pod wetted area	1.007	1.000
Estimated inlet pressure recovery	0.945	0.925
Relative inlet weight	0.727	1.00

Detail Nacelle Design and Integration Study

Nacelle Exterior Shape Study

A study was conducted to determine the best axisymmetric nacelle shape for the given wing-body configuration, nacelle location, and engine size. The range of possible nacelle shapes was constrained by the fixed inlet diameter, nacelle exit diameter, and nacelle length associated with a chosen engine size. The range of possible shapes was further constrained by a desire to have the nacelle cross-sectional area gradually increasing from the inlet to the wing trailing edge station. This expanding nacelle would create a compression region underneath the wing, increasing the wing lift with the nacelles installed. A family of uncambered nacelle shapes with varying maximum diameter was selected for study. A smallest maximum nacelle diameter was established as the minimum required for engine packaging.

An accompanying family of cambered nacelles was also studied. The camber distributions were chosen to keep the bottom external line of the nacelle straight from the compressor face to the nozzle exit and allow all of the cross-sectional area change to be taken on the nacelle upper surface. It was felt this would contribute to the favorable wing-nacelle inteference by strengthening the compression region on the top of the nacelle. Both families of nacelles are shown in Fig. 8.

Analysis of the nacelles consisted of determining the installed wave drag and drag due to lift for both the cambered and uncambered families. The installed wave drag was calculated using the wave drag program, and the installed drag due to lift was calculated using the McDonnell Douglas modified version of the Woodward[8] program and a linearized trim drag analysis. The induced drag analysis included the effects of wing reflexing to achieve favorable nacelle interference, at least to the first order.

Results of the analysis are also shown in Fig. 8. The cambered nacelle packaged as close as possible to the engine has the lowest total installed drag. The induced drag of the cambered nacelles increases as the nacelles maximum diameter increases because the camber of the nacelles is also increasing (see Fig. 8), and the drag increment due to the nacelle camber is growing rapidly.

An interesting byproduct of this analysis is a comparison of the isolated nacelle wave drags as calculated by the wave drag

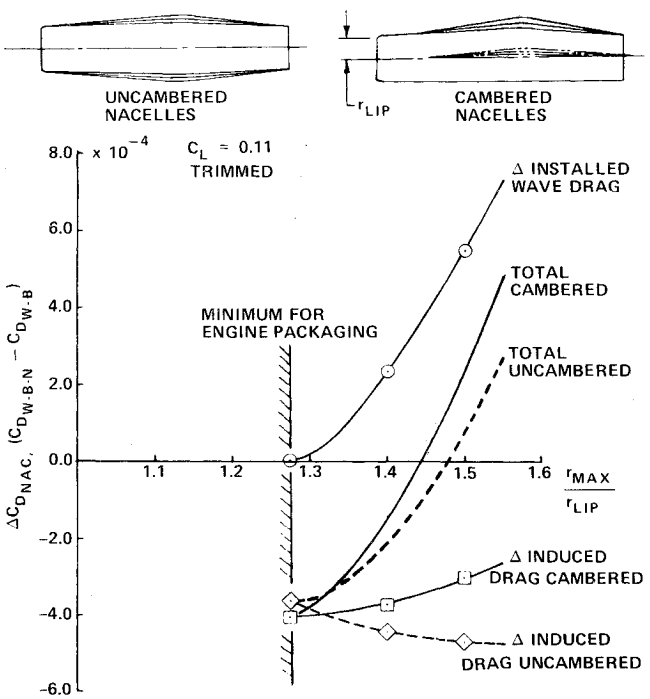

Fig. 8 Results of nacelle exterior shape study.

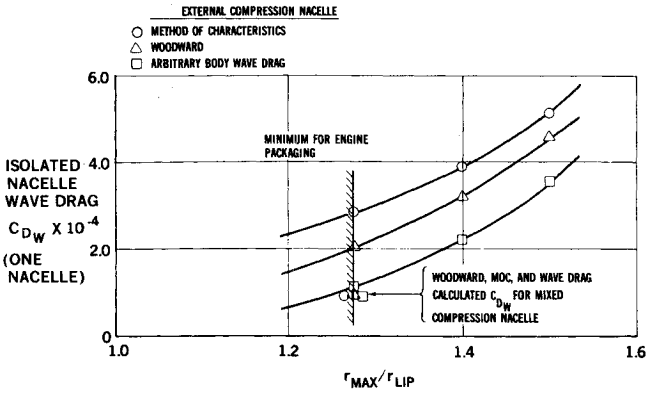

Fig. 9 Comparison of isolated uncambered nacelle wave drag as calculated by several methods.

program, the Woodward program, and the axisymmetric Method of Characteristics (MOC) program.[9] As shown in Fig. 9, the MOC program predicted more drag than the Woodward program, which predicted more drag than the wave drag program. The MOC is assumed to be correct because it is an exact solution and the differences in drag are attributed to the slender body and linearized far-field treatments of the external compression inlet lips by the Woodward and wave drag programs, respectively. Of particular interest is the fact that the wave drag theory cannot adequately address the drag on the external compression cowl lip. Knowing that the wave drag program does not correctly predict the isolated nacelle wave drag means that the installed wave drag cannot be accurately predicted. This problem is compounded by the knowledge that considerably fewer sampling planes are passed through the nacelle in the installed analysis than in the isolated analysis. However, the study does show that the drag program can adequately predict wave drag increments for changes in nacelle shape which are distributed over a substantial percentage of the length of the nacelle. This is indicated in Fig. 9 by the similarity in the variation of wave drag with maximum diameter predicted by each of the programs for the external compression nacelle and by the similarity in the wave drag calculated by each of the programs for the mixed compression nacelle. Consequently, although the actual installed wave drag levels cannot be accurately determined for the external compression nacelles, the wave drag increments due to the changes in overall shape are adequately predicted and the nacelle shape study results are considered to be valid.

At this point in the analysis, the unknown cowl-lip wave drag for the external compression inlet was expected to be high, but it was hoped that enough favorable wing-nacelle interference could be generated to offset the high cowl drag. It was felt that the strong lip shock and attendant high-pressure field would provide enough favorable interference to make the less complex external compression inlet the best overall choice. Therefore, the next detail design step was to develop a wing reflexed for the external compression inlet-nacelle.

Reflex Wing Design

Available linearized lifting surface methods were found to be inadequate to design the wing reflex for the external compression inlet-nacelle largely due to the inability to achieve a sufficiently detailed solution in the inlet-nacelle region and the inability to accurately model the strong cowl lip shock wave. Consequently, a wing reflexing technique using the MOC program was developed that could correctly model strong inlet shocks and permit sufficient detail to adequately define a reflex for the complicated multinacelle intersecting shock system.

The intent of the wing reflex is to return the pressure loading, ΔC_p, on the wing with nacelles installed to the pressure loading for the clean wing. This cancelling of the

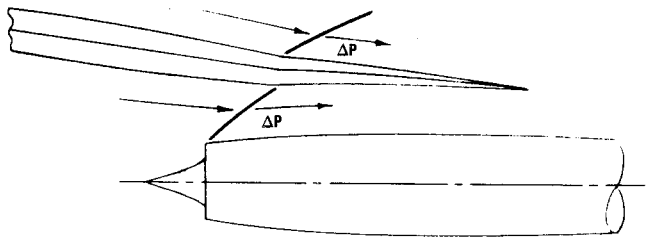

REFLEXING THE WING TO THE NACELLE FLOWFIELD DIRECTION CANCELS THE REFLECTED SHOCK (CAPTURES THE LIP SHOCK) AND RETURNS THE LOADING TO THE WING ALONE DISTRIBUTION BY INTRODUCING A COMPRESSION REGION ON THE WING UPPER SURFACE.

Fig. 10 Wing reflexing theory and procedure.

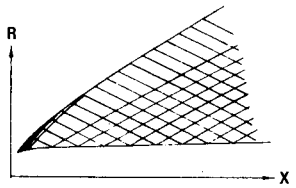

1. METHOD OF CHARACTERISTICS SOLUTION FOR THE AXISYMMETRIC NACELLE SHOCK WAVE AND FLOWFIELD

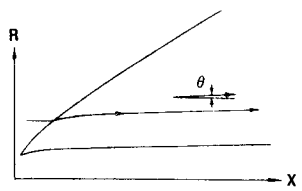

2. KNOWING THE LOCAL FLOW DIRECTION, θ, $dR/dX = \tan\theta$

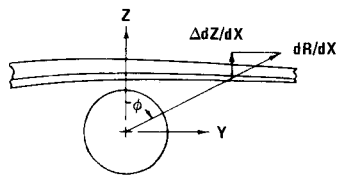

3. DETERMINE THE MAGNITUDE AND DIRECTION OF dR/dX ON THE UNREFLEXED WING LOWER SURFACE. THE ΔC_p DUE TO THE NACELLE IS CANCELLED BY REFLEXING BY THE AMOUNT $\Delta(dZ/dX) = (dR/dX)\cos\phi$

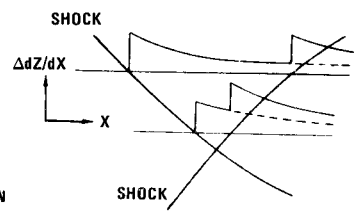

4. SHOCK WAVE INTERSECTIONS ARE MODELLED BY LINEAR ADDITION OF THE REFLEX $\Delta(dZ/dX)$

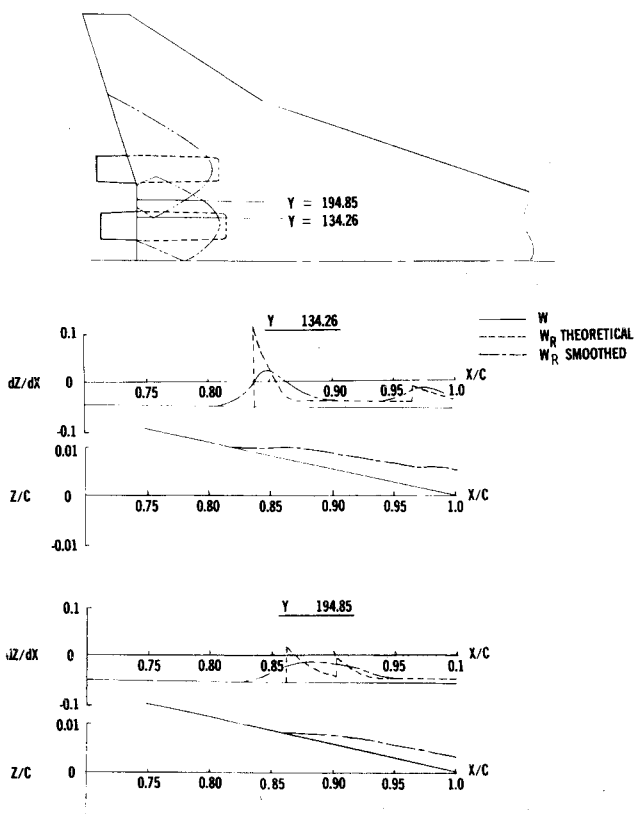

Fig. 11 Smoothing of wing camber slopes and resulting camber surface shapes.

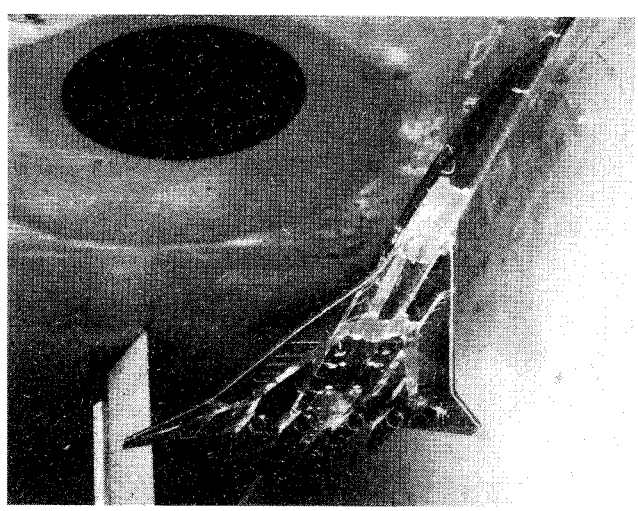

Fig. 12 High-speed model in NASA Ames 9- × 7-ft tunnel.

interference lift in the nacelle region is intended to keep the wing-body-nacelle pitching moments at the wing-body level. This permits the nacelles installed configuration to operate at cruise with significantly less trim drag with the reflexed wing because less tail download is required than with the unreflexed wing. The return to the wing-alone loading is accomplished by reflexing the wing camber surface to the nacelle flowfield direction, cancelling the lower surface reflected shock and returning the loading to the wing-alone distribution by introducing an equal strength compression region on the wing upper surface as shown in Fig. 10.

The theoretical reflex is shown in Fig. 11 indicating the required slope changes at the wing camber surface. Because of shock wave-boundary layer interaction, the exact location of the nacelle shock on the wing lower surface is expected to be upstream of the inviscid location and the shock pressure rise is expected to be distributed streamwise. Therefore, the theoretical camber slope peaks were smoothed out and slope discontinuities were eliminated. The smearing of the theoretical camber slopes and the resultant wing camber shapes are shown in Fig. 11.

At this point, the aerodynamic design and integration of the wing-body-nacelle combination was complete. The external compression inlet was more desirable because of simplicity and lower weight but, as shown, the installed drag penalty could not be accurately calculated. A wind-tunnel test appeared to be the only way to settle the inlet cowl-lip drag question and assess the effectiveness of the design and integration procedures developed during these studies.

Wind-Tunnel Test

A joint Douglas-NASA wind-tunnel test[§] of the configurations of interest was conducted at the NASA Ames

[§] This work was performed under NASA Contract NAS1-13633 and reported in Ref. 10.

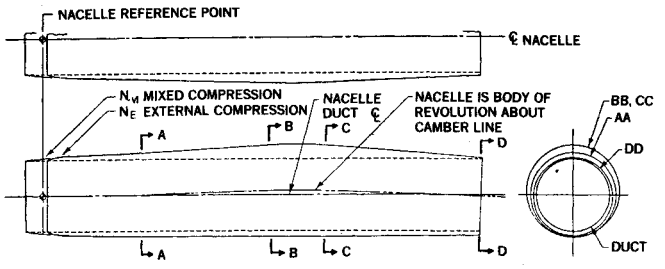

Fig. 13 Nacelles N_E and N_M.

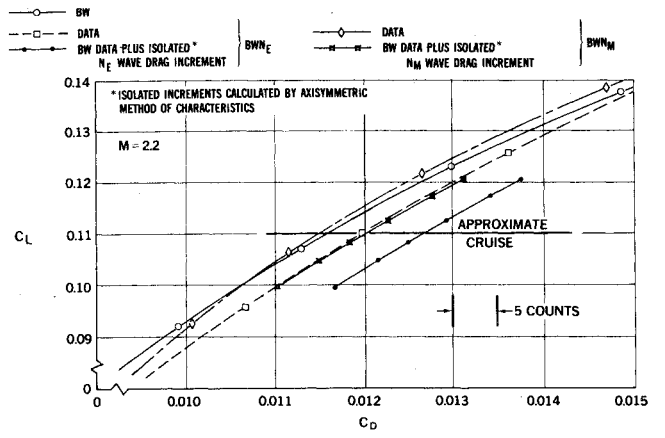

NOTE: A THIRD WING DESIGNED TO OPTIMIZE TRIMMED OPERATION WAS ALSO TESTED AND GAVE SUBSTANTIALLY BETTER TRIMMED L/D'S. THIS WORK IS THE SUBJECT OF REFERENCE 11.

Fig. 14 Comparison of untrimmed wing-body and wing-body-nacelle polars for the mixed and external compression nacelles.

facility. The test was funded as part of the NASA Supersonic Cruise Aircraft Research (SCAR) program originating at the NASA-Langley Research Center. Mach numbers from 0.5 to 1.3 were run in the NASA-Ames 11-×11-ft tunnel and Mach numbers from 1.6 to 2.4 were run in the NASA-Ames 9-×7-ft tunnel.

Model scale was 0.015 based on a full-scale wing area of 10,000 square feet, and all data were taken at a Reynolds number of 4.0×10^6 per ft which corresponds to a model Reynolds number of 3.9×10^6 based on the wing trapezoidal MAC of 0.973 ft. A picture of the model installed in the NASA-Ames 9-×7-ft tunnel is shown in Fig. 12.

The model parts[¶] consisted of the baseline fuselage (B) optimized for minimum wave drag in the presence of the nacelles and baseline wing; the baseline wing (W) optimized using Woodward for minimum induced drag; the reflexed wing (W_R); and an external compression nacelle (N_E) and mixed compression nacelle (N_M) illustrated on Fig. 13.

The nacelles were flow-through with no centerbody spike. The internal contours were constant diameter, straight bores so that accurate force data corrections could be made. The test data have been corrected, using analytic methods, to flight conditions for the aircraft configuration with a closed afterbody. Corrections were made for the changes in skin friction drag wave drag, and drag due to lift. The nacelle external skin friction drag was removed from the data. Unless otherwise stated, the discussion of test results will pertain to the cruise design point, $2.2M$, $C_L = 0.11$.

The results of installing either nacelle on the baseline wing are shown on Fig. 14. There is a drag reduction (relative to the wing body) of 0.9% for N_M and a drag penalty of 3.4% for

[¶]An additional wing constrained to optimize trimmed operation was also tested, and showed substantially better L/D's than either the baseline or reflexed wing. These results are not included in this paper because they do not assist in understanding the nacelle installation problem. Discussion of the design and testing of this trim optimized wing is the subject of Ref. 11.

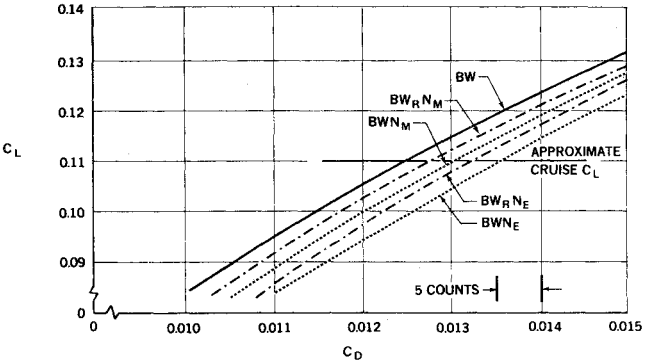

Fig. 15 Effect of wing reflexing on trimmed wing-body-nacelle polars with mixed and external compression nacelles, $M = 2.2$.

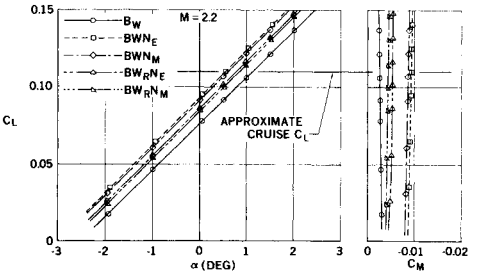

Fig. 16 Lift curves and pitching moments for the wing-body and wing-body-nacelle combinations.

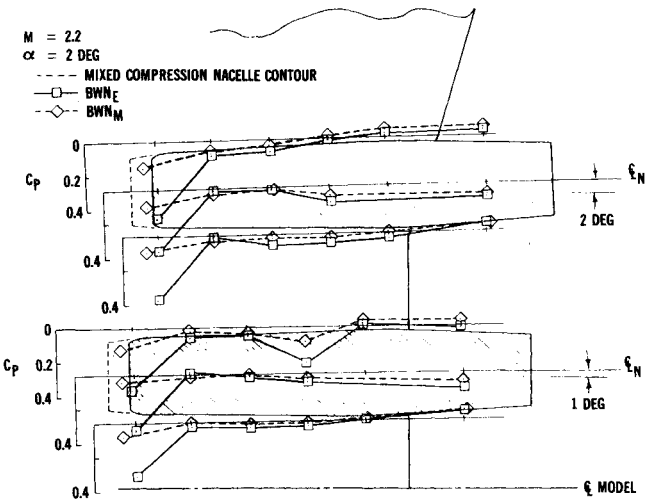

Fig. 17 Installed nacelle pressure distributions.

N_E. Also shown is the increment in drag calculated by the MOC program. The drag increment between the nacelles predicted by the MOC is almost the same as the increment measured experimentally implying that the installation drag penalty for the external compression nacelle is due to the inlet lip drag.

The nacelle incremental drags were slightly greater for the untrimmed reflexed wing. However, when the data are trimmed, then the reflexed wing has a favorable benefit of 2.6-3.0% relative to the baseline wing as illustrated on Fig. 15. Reflexing the wing alleviates some of the aft loading caused by the nacelle installation thereby producing more positive pitching moments and less tail down load to trim the aircraft. The pitching moments and less tail down load to trim aircraft. The pitching moments and lift curves are shown for all configurations on Fig. 16.

The preceding figures also illustrate that the external compression nacelle has about 4.3% more drag than the mixed compression nacelle and that the drag reduction due to the trimmed, reflexed wing was the same for either nacelle.

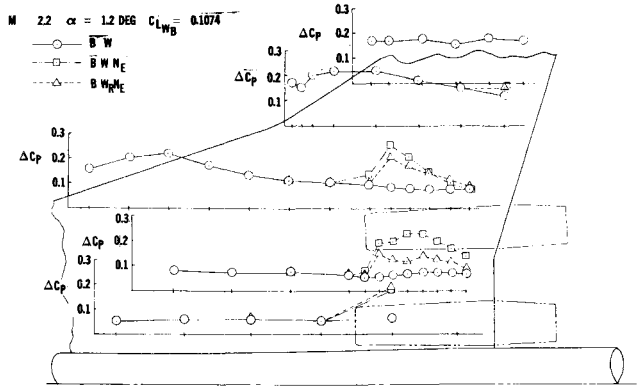

Fig. 18 Wing pressure loading, ΔC_P, with external compression nacelles.

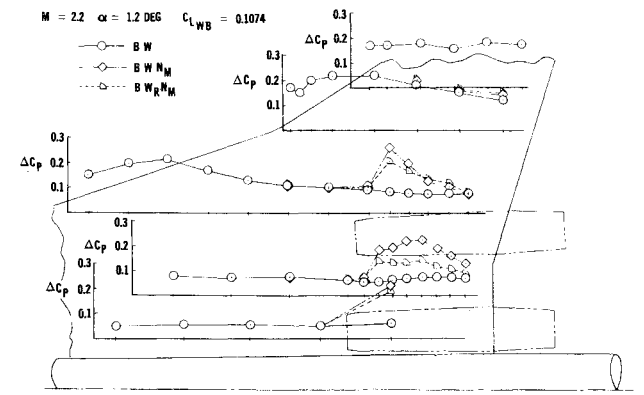

Fig. 19 Wing pressure loading, ΔC_P, with mixed compression nacelles.

The pressure distributions on the installed nacelles and the wing loadings are shown on Figs. 17-19. The higher pressure in the lip region of N_E is illustrated on Fig. 17. However, by comparing Figs. 18 and 19, this higher lip pressure does not appear in the wing loadings due to radial attenuation away from the nacelle or due to shock boundary interaction effects. Since little of the higher pressure that exists on the lip producing drag appears on the wing, there is a small potential of ever achieving cancellation of the drag by favorable interference and wing reflexing for an external compression inlet.

Aside from the lip pressure considerations, the reduction in aft loading mentioned earlier is illustrated on either Fig. 18 or 19. It is felt that the pressure loadings do not return to wing-alone levels because of the complexity of the flow in the nacelle region. The three-dimensionality of the boundary-layer diverter channel flows and shock-wave intersections, impingements, and boundary-layer interactions could not be considered in the reflex design and undoubtedly accounts for some of the difference in loadings. The location of the inlet lip shock upstream of its predicted inviscid location, as shown in Fig. 20, is a good illustration of the consequence of these effects. The shock pressure rise moved upstream roughly one boundary-layer height.

It seems that wing reflexing can be satisfactorily accomplished by the use of a more generalized reflex aimed at tailoring the wing-body-nacelle pitching moments to give reduced trim drag. An example of a generalized reflex would be a wing reflexed by a constant $\Delta(dZ/dX)$ over the entire wing region affected by the nacelles. Should an economic three-dimensional analysis scheme make sophisticated design studies possible, a generalized reflex may still be preferable to a point design because a generalized reflex with less severe slope changes would be expected to have smaller drag penalties at off design Mach numbers.

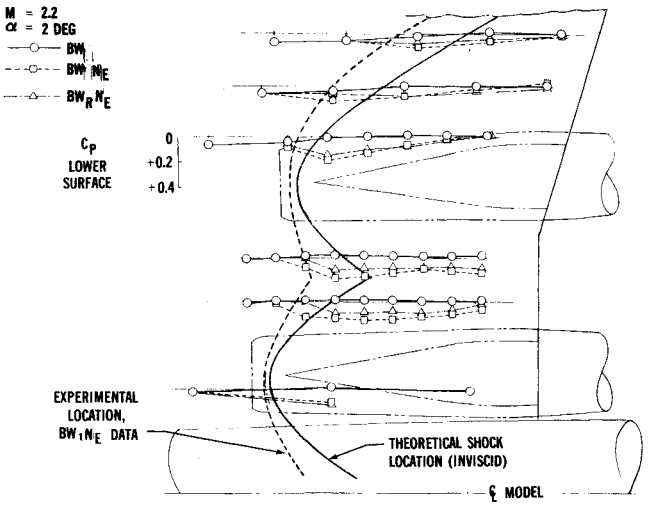

Fig. 20 Lower surface pressure distributions showing the effect of wing reflexing and the location of the inlet shock impingement.

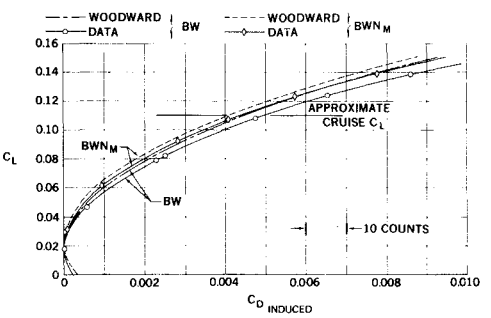

Fig. 21 Comparison of Woodward calculated and experimentally determined induced drag for the wing-body and wing-body with mixed compression nacelle, $M = 2.2$.

A comparison of the Woodward-calculated induced drag with the test data is shown in Fig. 21 for the wing-body and the wing-body with mixed compression nacelles installed. It can be seen that at 2.2M the Woodward has underpredicted the induced drag slightly but has accurately predicted the drag increment between the wing-body and wing-body-nacelle configurations.

Conclusions

The general conclusions not necessarily tied to the specific configurations of this program, but drawn from the overall result of this work are as follows:

1) The single-engine axisymmetric pods are clearly aerodynamically superior to the dual-engine two-dimensional pods because the total nacelle cross-sectional area is less and the 2.2M projected nacelle area can be better distributed in each of the area rule roll angles so as to achieve a low wave drag configuration.

2) The full isolated wave drag increment between the mixed and external compression inlets was observed at 2.2M. The implication is that for axisymmetric nacelles located out of the boundary layer, the full isolated cowl lip wave drag can be expected in addition to any favorable interference between the wing and nacelles.

3) For axisymmetric nacelles, the benfits of wing reflexing are achieved via improvement of configuration trim drag rather than by improvement of the untrimmed drag due to lift.

4) Future reflex designs do not have to capture all the details of the specific installation flowfield to be effective. Reflexing should be aimed at tailoring the wing-body-nacelle pitching moments to give reduced trim drag. A constant slope reflex may well be adequate for this purpose.

5) Linearized analysis methods are inadequate for dealing with the high rates of change of cross-sectional area and strong shock waves associated with external compression inlets at 2.2*M*. The area rule theory and Woodward program are, however, more than adequate for designing a wing nacelle installation with mixed compression inlets.

References

[1] FitzSimmons, R.D. and Hoover, W.C., "AST—A Fifth Engine for Environmental Consideration," SAE Paper 730899, 1973.

[2] "Studies of the Impact of Advanced Technologies Applied to Supersonic Transport Aircraft," Douglas Report MDC J4394, 1973.

[3] FitzSimmons, R.D. and Roensch, R.L., "Advanced Supersonic Transport," SAE Paper 750617, 1975.

[4] Sovran, G. (ed.), "Fluid Mechanics of Internal Flow," Elsevier, New York, 1967.

[5] Gentry, A.E., Smyth, D.N., and Oliver, W.R., "The Mark IV Supersonic-Hypersonic Arbitrary-Body Program," AFFDL-TR-73-159, 1973.

[6] Jones, R.T., "Theory of Wing-Body Drag at Supersonic Speeds," NACA RM A53H18a, 1953.

[7] Whitcomb, R.T., "A Study of Zero-Lift Drag Rise Characteristics of Wing-Body Combinations Near the Speed of Sound," NACA RM L52H08, 1952.

[8] Woodward, F.A., Tinoco, E.N., and Larsen, J.W., "Analysis and Design of Supersonic Wing-Body Combinations, Including Flow Properties in the Near Field," NASA CR-73106, 1967.

[9] Henne, P.A., "Unique Applications of the Method of Characteristics to Inlet and Nozzle Design Problems," AIAA Paper 75-1185, 1975.

[10] Radkey, R.L., Welge, H.R., and Felix, J.E., "Aerodynamic Characteristics of a Mach 2.2 Advanced Supersonic Cruise Aircraft Configuration at Mach Numbers from 0.5 to 2.4," prepared by Douglas Aircraft Company under NASA Contract NAS1-13633, NASA CR-145094, Feb. 1977.

[11] Radkey, R.L., Welge, H.R., and Roensch, R.L., "Aerodynamic Design of a Mach 2.2 Supersonic Cruise Aircraft," AIAA Paper 76-955, 1976.